Saudi Journal of Biological Sciences 29 (2022) 3918–3928

Contents lists available at ScienceDirect

Saudi Journal of Biological Sciences

journal homepage: www.sciencedirect.com

Original article

Screening of rice cultivars for Cr-stress response by using the parameters of seed germination, morpho-physiological and antioxidant analysis

Farwa Basit [a,b], Javaid Akhter Bhat [c,*], Jiajun Han [b], Yajing Guan [a,b,*], Basit Latief Jan [d], Awais Shakoor [e], Saleh Alansi [f]

[a] Hainan Research Institute, Zhejiang University, Sanya, 572025, China
[b] Seed Science Center, Institute of Crop Sciences, College of Agriculture and Biotechnology, Zhejiang University, China
[c] International Genome Centre, Jiangsu University, Zhenjiang 212013, China
[d] Department of Clinical Pharmacy, College of Pharmacy, King Saud University, Riyadh 11451, Saudi Arabia
[e] Department of Environment and Soil Sciences, University of Lleida, 25198 Lleida, Spain
[f] Botany and Microbiology Department, College of Science, King Saud University, 11451 Riyadh, Saudi Arabia

ARTICLE INFO

Article history:
Received 9 January 2022
Revised 20 February 2022
Accepted 21 February 2022
Available online 4 March 2022

Keywords:
Seed germination
Photosynthesis
Oxidative damage
Rice
Hydroponic screening
Stress tolerance

ABSTRACT

Rice is the most important crop for the majority of population across the world with sensitive behavior toward heavy metals such as chromium (Cr) in polluted regions. Although, there is no information on the Cr resistance phenotyping in rice. Herein, two different groups of rice cultivars (normal, and hybrid) were used, each group with 14 different rice cultivars. Firstly, seed germination analysis was conducted by evaluating various seed germination indices to identify the rice cultivars with greatest seed germination vigor. Furthermore, exposure of chromium (Cr) toxicity to 28 different rice varieties (NV1-NV14, HV1-HV14) caused noticeable plant biomass reduction. Subsequently, NV2, NV6, NV10, NV12, NV13 (normal type), HV1, HV4, HV8, and HV9 (hybrid types) were pragmatic as moderately sensitive varieties, while NV3, NV4, NV9, and NV14 (normal type), HV3, HV6, HV7, and HV13 were observed as moderately tolerant. Although, NV7, and HV10 were ranked most sensitive cultivars, and NV11, and HV14 were considered as most tolerant varieties as compared to the other rice (both groups) genotypes. Afterward, Cr induced reduction in chlorophyll pigments were significantly lesser in HV14 relative to NV11, NV7, and especially HV10, and as a result HV14 modulated the total soluble sugar level as well as reduced ROS accumulation, and MDA contents production by stimulating the antioxidant defense mechanism conspicuously which further reduced the electrolyte leakage as well. Our outcomes provide support to explore the Cr tolerance mechanism in cereal crops as well as knowledge about rice breeding with increased tolerance against Cr stress.

1. Introduction

Rice (*Oryza sativa* L.) an edible food crops, which is staple food by more than half of human population world widely (Gross and Zhao, 2014). About 40,000 of rice varieties have been introduced world widely, and these varieties are different in yield production, toward adaptation of environmental alternations, agro-ecological changes, tolerance mechanism toward pest, disease, and environmental stresses (Chhogyell et al., 2016). Several investigations demonstrated that the rice varieties differ across various ecological regions, and few cultivars perform highly significant yield production as compared to different genotypes under varying environmental conditions (Moorthy et al., 2011; Mosavi et al., 2013). It is considered that hybrid rice cultivars can adopt environmental alterations, and farming systems i.e. System of Rice Intensification (SRI) quickly as comparable to the normal rice types, and therefore, improved rice growth, and biomass is noticed in hybrid rice cultivars than normal rice varieties (Thakur et al., 2015). Nevertheless, the increasing soil contamination especially heavy metals (HMs)

* Corresponding authors at: Hainan Research Institute, Zhejiang University, Sanya, 572025, China (Y. Guan); International Genome Centre, Jiangsu University, Zhenjiang 212013, China (J. Akhter Bhat).

E-mail addresses: javid.akhter69@gmail.com (J. Akhter Bhat), vcguan@zju.edu.cn (Y. Guan).

Peer review under responsibility of King Saud University.

Production and hosting by Elsevier

https://doi.org/10.1016/j.sjbs.2022.02.038
1319-562X/

pollution is becoming a major concern for plant researcher society (Wakeel et al., 2021). Moreover, HMs are accumulated inside edible food parts (Chen et al., 2022), and further become the risk for humans, and animals health (Shen et al., 2017). Amongst HMs, the chromium (Cr) is known as most persuasive pollutant inside ecosystem (Gill et al., 2016), which comprises a particular density 7.19 g/cm^3, ranked 7th inside most abundant metal as well as 21st most abundant HMs on the earth (Economou-Eliopoulos et al., 2014). The Cr contains different oxidative states (O-V1), but the Cr (III), and Cr (VI) are deliberated as the most stable form (Singh et al., 2021). However, the Cr (VI) has more mobile, toxic, mutagenic, and carcinogenic nature than Cr (III) (Ashraf et al., 2017; Geng et al., 2019). Plants use phosphate, and Sulphur pathway to uptake Cr through roots. Hence, it is translocated into the other plant's parts (Xu et al., 2018). Whereas, roots act as prime organs to in contact with Cr contaminated soil, and play primary role in uptake, accumulation, and translocation of Cr (Al-Huqail et al., 2020; Karthikeyan et al., 2020).

Cr cause severe phytotoxic effects on plants growth, and biomass by decreasing the photosynthetic rate, disturbing mineral uptake balance, and increasing Cr uptake (Singh et al., 2021). It is noticed that Cr stress cause reduction in seed germination rate, and disturb the antioxidative defense mechanism as well (Basit et al., 2021a; Basit et al., 2021c; Basit et al., 2022). It is revealed that Cr uptake, and translocation minimize the germination, and growth ratio, negatively effects on chlorophyll pigments production, and PSII system, and increase electrolyte leakage by stimulating the ROS generation (Wakeel et al., 2020), and ultimately crop yield is compromised. Furthermore, the plants uptake Cr through Cr contaminated nutrient solution by using roots, which resultant numerous morpho-physiological, biochemical, and molecular changes as well (Farid et al., 2019; Islam et al., 2019). In another study, it is noticed that nutrient, and Cr uptake competition cause Cr binding with carrier channels and plasma membrane, and weakened the H^+ ATPase activity (Habiba et al., 2019). A current study represented that Cr-induced phytotoxicity reduce plants biomass, and photosynthetic ability by enhancing the stress markers such as malondialdehyde (MDA), and hydrogen peroxide (H_2O_2), electrolyte leakage (EL), and Cr uptake inside *Oryza sativa* (Basit et al., 2021a), *Sesbania sesban* (Din et al., 2020), *Brassica napus* (Ulhassan et al., 2019b), tomato (Alamri et al., 2020), *Spinacia oleracea* (Zaheer et al., 2020).

In addition, Cr accumulation cause cellular structure damage which further increase the cellular oxidative damage by triggering the ROS over-production such as MDA, H_2O_2, and EL (Patra et al., 2019). Higher ROS accumulation cause membrane peroxidation of lipids, interruption of membrane organization and function, beside the oxidation of cellular macromolecules such DNA and proteins (Farid et al., 2017; Wakeel et al., 2019; Basit et al., 2022). To overcome the adverse effects of ROS production, and accumulation, plants develop a specific mechanism named as antioxidative defense system that includes both enzymatic and non-enzymatic (Zaheer et al., 2020; Kharbech et al., 2022). Although, Cr-toxicity also affects the antioxidant activities as well (Ulhassan et al., 2019b; Wakeel et al., 2020). In general, Cr stress alter the biochemical, and physiological attributes of rice cultivars, and consequently lead to the growth inhibition, and crops yield loss (Singh and Prasad, 2019; Basit et al., 2021a; Sharma et al., 2022).

A recent study was designed to observe the seed germination ratio and various germination indices rates of different rice varieties. Moreover, the determination of response differences related to biomass between hybrid, and normal types of rice varieties with, and without Cr toxicity at the seedling stage was hypothesized. Afterward, on the basis of the above-mentioned parameters, the most tolerant (H-V14, N-V11), and sensitive varieties (H-V8, N-V7) were selected, and Cr- induced toxicity was examined by measuring the photosynthetic pigments, electrolyte leakage, ROS generation, and antioxidative defense mechanism with/without Cr exposure. Although, the selection of more tolerant cultivars against Cr stress is the most sustainable solution to improve the plants growth, and yield in Cr contaminated soils. Herein, the main objective was to categorize the rice cultivars on the basis of their degree of tolerance, and sensitive nature under Cr-exposure.

2. Materials and methods

2.1. Plant materials

Current research used 14 different varieties of normal genotype, and 14 different genotypes of hybrid (total 28 cultivars of rice) were used to screen the sensitive, and tolerant cultivars. This all the plant material are collected from the Zhejiang Nongke Seeds CO., LTD. Hangzhou, China.

2.2. Seed germination analysis

Initially, the seeds were sterilized by using solution of NaOCl at 5% (w/v) for 15 min, and slightly washed through the water to eradicate the remaining chloride. To conduct the seed germination analysis, a box of size 12 × 18 cm in which 30 seeds in four replicates were germinated. Seed germination are conceded under controlled conditions by maintaining the temperature of 25 °C with a fluctuation cycle of 8 h brightness and 16 h darkness for 14 days in a growth chamber (Zheng et al., 2006). The 100 μM Cr was disclosed to the incubated seeds. Concentration of the Cr used are based on pre-experiments, which showed that the 100 μM Cr can significantly inhibit the seed germination ratio, and plant's growth and biomass as well plant damage/death.

The germinated seeds were counted at day 5th, and considered as germination energy (G.E). In addition, seeds counted on 14th day were deliberated as germination percentage (G.P). Germination index (G.I), vigor index (V.I), and mean germination time (MGT) are estimated by using the procedure as described in detail by (Zheng et al., 2006).

2.3. Plant growth conditions

The 100 μM concentration of $K_2Cr_2O_7$ with a nutrient media solution was exposed to the incubated seeds. Nutrient solution contains 0.5 μM potassium nitrate (KNO_3), 0.5 μM magnesium sulfate ($MgSO_4$), 2.5 μM Monopotassium phosphate (KH_2PO_4), 0.5 μM Calcium nitrate ($Ca(NO_3)_2$), 2.5 μM ammonium chloride (NH_4Cl), 100 μM ferric EDTA (Fe–K–EDTA), 30 μM H_3BO_3, 1 μM zinc sulfate ($ZnSO_4$), 5 μM manganese monosulfate ($MnSO_4$), 1 μM copper(II) sulfate ($CuSO_4$), and 1 μM ammonium heptamolybdate ($(NH_4)_6$-Mo_7O_{24}) per liter. The nutrient media solution was adjusted at pH 5.0 with the assistance of HCl, and NaOH.

2.4. Experimental design

Hydroponic solution was used to perform the experiment. The 100 μM Cr concentration was treated with two-week-old seedlings, and the seeds not treated with Cr deliberated as control (CK). The completely randomized design (CRD) statistical method was followed to carry out the experiment, and relocation of the in the growth chamber was done each day. Collection of the samples for the estimation of various growth parameters was carried out at 21 days.

2.5. Plant growth investigations

The plants were immersed after harvesting into the ddH_2O containing bucker to eliminate the remains of disinfectant and scrutinize the safety of roots. The plant length (PL) was measured using the ruler and measured the fresh weight (FW). The dry weight (DW) of plants was calculated after drying it inside the oven at 80 °C for 24 h.

2.6. Determination of chlorophyll pigments

The chlorophyll contents i.e. chlorophyll *a*, b, a + b, and carotenoids are estimated by using method of (Lichtenthaler and Wellburn, 1983). In brief, 0.2 g fresh leaves samples were homogenize in 3 mL ethanol (95%, v/v), and the centrifugation of the homogenized samples were done at 5000 × g for 10 min and, then, supernatant was obtained. Furthermore, supplementation of 9 mL ethanol (95%, v/v) was carried out with a 1 mL aliquot of the supernatant. Then after, the calculations were conceded at the 665, 649, and 470 nm through using spectrophotometer (UV-1900, Shimadzu, Japan).

2.7. Total soluble sugar and electrolyte leakage estimation

Estimation of soluble sugar (total), 0.5 g fresh and health tissue of leaf were ground in pestle and mortar beside with extraction buffer in it. Phosphate buffer (50 mM, pH 7), glycerol (10%, v/v), ascorbate (1 mM), KCl (100 mM) and β-mercaptoethanol (5 mM) was used for the preparation of extraction buffer. Then, the homogenate was assembled into the microcentrifuge tube through 15 min centrifugations at 12,000 g. Far along, precipitate are used for quantification of soluble sugar (total) through following the phenol–sulfuric acid assay (Dubois et al., 1951).

To estimate the electrolyte leakage as EL (dSm^{-1}), surface sterilization was conducted by 5 g seeds with $HgCl_2$ (1%), and speckled with ddH_2O using at least four replications. Subsequently, seedlings were soaked into the 25 mL ddH_2O as well as incubated (25 °C) for 24 h. The sample was moved to alternative blank beaker and ddH_2O was added up to 25 mL volume, EL was stated in dSm^{-1} deliberating to the previous rule (Ista et al., 2004).

2.8. Quantification of MDA, H_2O_2 and $O_2^{\bullet -}$ contents

Estimation of MDA contents are performed by utilizing the 2-thiobarbituric acid (TBA), tissue extract (1.5 mL), and homogenized in 5% TBA (2.5 mL), and diluted inside 5% $C_2HCl_3O_2$. Far along, homogenized samples are boiled at 90 °C for 20 min and earlier cooled it at ice instantaneously, and centrifuged at 5000 × g for 10 min, and the readings are taken at 532 and 600 nm wavelengths via using UV–vis spectrophotometer (Hitachi U-2910) (Heath and Packer, 1968). The value of MDA content was stated as nmol mg^{-1} protein.

The H_2O_2 was measured by using the plant tissues (homogenized) in phosphate buffer and centrifuged at 6000 g. The 0.1% titanium sulfate containing 20% (v/v) H_2SO_4 was added into obtained supernatant and intermixed. The yellowness intensity was observed at 410 nm via calorimetrically (Kwasniewski et al., 2013). The contents of H_2O_2 were quantified by constructing the standard curve, and for this the H_2O_2 and reaction mixture known concentration without plant tissue was considered as control along with its observations subtracted from treatments. The H_2O_2 contents are estimated at at 25 ± 2 °C in term of (μmol g^{-1} FW).

Superoxide radical ($O_2^{\bullet -}$) was quantified according to the protocol of Jiang and Zhang (2001) with minor modifications. Around 0.5 g of plant tissues were intermixed in 4 mL of 70 mM K_3PO_4 buffer, and thereafter around 12 min this mixture was centrifuged at 5000 g. One mL supernatant was intermixed with 0.8 mL of 70 mM K_3PO_4 buffer and 0.2 mL of 10 mM $HONH_2{\cdot}HCl$. Afterward, the mixture was incubated for 24 h. Then, 1 mL of sulphanilamide (17 mM) and anaphthylamine (7 mM) were mixed for 20 min at 25 °C. The 1 mL of n-butanol was supplemented after incubation, and further centrifuged for around 10 min at 15,000 g. The absorbance was testified at 530 nm and generation rate of superoxide radical was measured with standard curve.

2.9. Determination of antioxidant enzyme activities

The supernatant taken from total soluble sugar was also used to estimate activities of antioxidants. To perceive the activity of SOD (superoxide dismutase) the protocol of El-Shabrawi et al. (2010) was followed. The changes within the reaction mixture absorbance counting 50 mM K_3PO_4 buffer, 2.24 mM $C_{40}H_{30}Cl_2N_{10}O_6$, 2.36 mM $C_5H_4N_4O_2$ and 0.1 units xanthine oxidase were testified for 2 min. One unit of SOD activity was assayed as unit (min^{-1} mg^{-1} protein) followed by enzyme quantity needed required to restrict NBT reduction (50%). Extinction coefficient of 39.4 M^{-1} cm^{-1} are utilized to calculate the catalase (CAT) activity according to the protocol of (Hossain et al., 2010). The POD (peroxidase) activity was assayed followed the Change and Maehly (1955) methodology, and enzyme activity was estimated as l M of guaiacol oxidized g^{-1} FW min^{-1} at 25 ± 2 °C. Activity of APX activity are estimated by relying on reduction taken at 290 nm absorbance, as the oxidation of the as ascorbate occurs. Reaction mixture of 3 mL containing 2.7 mL, 0.1 mL, 0.1 mL and 0.1 mL of PO_4^{3-} buffer (25 mM, pH 7.0), ascorbate (7.5 mM), 0.1 H_2O_2 (0.4%) and 0.1 mL enzyme extract, respectively. The reaction commenced after mixing H_2O_2. The activity of enzyme was deliberated as μ mol min^{-1} mg^{-1} protein at 25 ± 2 °C (Nakano and Asada, 1981).

2.10. Statistical analysis

The One-way ANOVA was used in all experimental data, and the least significant differences (LSD) was calculated at $p < 0.05$ and $p < 0.01$ levels between mean values using Statistix (8.1) software. Four replications are used in each experiment.

3. Results

3.1. Estimation of seed germination indices of different rice types

In a recent investigation, two different categories of rice types (Normal, and hybrid), 14 various varieties of normal, and 14 different types of hybrid cultivars were selected to identify the seed germination parameters by conducting different seed germination parameters such as G.E, G.P, V.I, G.I, and M.G.T under normal condition. The outcomes revealed that HV3, HV5, HV10, and HV14 (hybrid varieties), and NV7, NV8, NV11, and NV14 (normal varieties) represented the more obvious results related to G.E, G.P. G.I, and V.I, with less M.G.T as compared to the other rice varieties (Tables 1, 2). However, more betterment was observed in hybrid type varieties as compared to the normal types of rice genotypes in respect to the seed germination analysis. In addition, HV5, HV14 and NV11 had 100% G.P and showed significantly greater G.E as compared to the other genotypes of both rice types. However, HV3, HV14, NV14, and NV11 demonstrated significantly lower M.G.T (Tables 1, 2). In the control condition, the HV11, HV8, NV1, NV5, and NV6 confirmed lower values for seed germination indices, such as G.E, G.P, G.I, and V.I, and revealed greater M.G.T values, particularly in HV2, HV9, HV11, NV1, and NV6 (Tables 1, 2). On the bases of seed germination parameters, our results declared that as comparable to other varieties, NV7, NV11, NV12, NV14 from

Table 1
Seed germination analysis of 14 different cultivars of normal rice type. germination energy (%), germination percentage (%), germination index (%), mean germination time (%), and vigor index (%) under normal condition.

Varieties	GE (%)	GP (%)	GI	MGT	VI
NV1	76.25 ± 4.79 g	76.25 ± 2.50d	4.29 ± 0.15 g	3.77 ± 0.13a	0.40 ± 0.02 g
NV2	83.75 ± 4.79ef	85.00 ± 4.08bc	6.54 ± 0.26f	3.19 ± 0.08bc	0.88 ± 0.03f
NV3	88.75 ± 6.29bcde	96.55 ± 4.79b	6.89 ± 0.22f	2.85 ± 0.11d	1.04 ± 0.11e
NV4	93.75 ± 4.79ab	97.50 ± 5.00b	6.94 ± 0.14f	2.72 ± 0.12d	1.13 ± 0.04e
NV5	77.50 ± 2.89 fg	81.25 ± 2.50 cd	7.34 ± 0.68f	3.10 ± 0.12c	0.80 ± 0.03f
NV6	77.50 ± 5.00 fg	88.75 ± 4.79b	6.82 ± 0.59f	3.39 ± 0.20b	0.86 ± 0.07f
NV7	94.75 ± 7.50ab	98.75 ± 2.50ab	13.90 ± 0.37bc	2.19 ± 0.3ef	1.78 ± 0.05c
NV8	92.50 ± 6.45abc	96.75 ± 4.79b	13.83 ± 1.24c	2.00 ± 0.19 fg	1.26 ± 0.01d
NV9	92.50 ± 2.89abc	97.50 ± 2.89b	9.32 ± 0.42de	2.80 ± 0.07d	1.09 ± 0.05e
NV10	86.25 ± 2.50cde	87.50 ± 2.89b	8.69 ± 0.39e	2.66 ± 0.15d	1.02 ± 0.04e
NV11	96.25 ± 4.79a	100.00 ± 0.00a	15.66 ± 0.58a	1.85 ± 0.17 g	2.25 ± 0.20a
NV12	91.25 ± 4.79abcd	95.90 ± 4.08b	13.60 ± 0.52c	2.38 ± 0.19e	1.03 ± 0.07e
NV13	85.00 ± 4.08de	97.50 ± 2.89b	9.60 ± 0.26d	2.10 ± 0.26f	0.38 ± 0.02 g
NV14	95.00 ± 4.08ab	98.75 ± 2.50ab	14.68 ± 1.11b	1.91 ± 0.10 fg	2.10 ± 0.14b

The same letters within a column designate there was no significant difference at a 95% probability level at the $p < 0.05$ level, correspondingly.

Table 2
Seed germination analysis of 14 different cultivars of hybrid rice type. germination energy (%), germination percentage (%), germination index (%), mean germination time (%), and vigor index (%) under normal condition.

Varieties	GE (%)	GP (%)	GI	MGT	VI
HV1	91.25 ± 2.50 cd	95.00 ± 4.08bc	8.22 ± 0.36e	2.55 ± 0.11 fg	0.56 ± 0.02 fg
HV2	96.25 ± 4.79abc	97.50 ± 2.89abc	7.29 ± 0.30 g	3.06 ± 0.09bc	0.68 ± 0.02e
HV3	95.00 ± 5.77abc	98.50 ± 2.89ab	15.39 ± 0.71b	1.87 ± 0.17 h	2.26 ± 0.10b
HV4	78.75 ± 2.50f	81.25 ± 2.50d	6.43 ± 0.08 h	2.81 ± 0.17cde	0.56 ± 0.02 fg
HV5	98.75 ± 2.50a	100.00 ± 0.00a	10.02 ± 0.43c	2.21 ± 0.09 h	0.94 ± 0.03c
HV6	92.50 ± 2.89bcd	93.75 ± 4.79c	7.65 ± 0.41efg	2.74 ± 0.18def	0.84 ± 0.06d
HV7	88.75 ± 2.50de	95.00 ± 4.08bc	8.01 ± 0.43ef	2.77 ± 0.23def	0.82 ± 0.05d
HV8	81.25 ± 6.29f	85.00 ± 5.77d	7.35 ± 0.66 fg	2.70 ± 0.27ef	0.58 ± 0.05f
HV9	93.75 ± 2.50abcd	97.50 ± 2.89abc	7.26 ± 0.15 g	3.08 ± 0.15b	0.82 ± 0.04d
HV10	97.50 ± 2.89ab	98.75 ± 2.50ab	9.28 ± 0.31d	2.28 ± 0.11 h	0.79 ± 0.04d
HV11	68.75 ± 2.50 g	76.25 ± 2.50e	5.12 ± 0.74i	3.62 ± 0.34a	0.49 ± 0.07 g
HV12	93.75 ± 4.79abcd	97.50 ± 5.00abc	7.69 ± 0.54efg	2.95 ± 0.09bcde	0.67 ± 0.05e
HV13	83.75 ± 2.50ef	83.75 ± 2.50d	6.40 ± 0.46 h	2.99 ± 0.15bcd	0.55 ± 0.03 fg
HV14	98.75 ± 2.89a	100.00 ± 2.50a	17.32 ± 0.86a	1.73 ± 0.19 h	2.37 ± 0.12a

The same letters within a column designate there was no significant difference at a 95% probability level at the $p < 0.05$ level, correspondingly.

group of normal rice type, and HV3, HV5, HV10, and HV14 from hybrid rice cultivars showed maximum germination ratio, with higher germination vigor as well as minimum germination time.

3.2. Effect of chromium toxicity on biomass of different rice types

Under control environment, NV4, NV6, NV7, NV8, NV9, NV11, and NV14 declared the higher plant biomass fresh, and dry weight (FW, DW), plant shoot, and root length (SL, RL) as comparable to the other genotypes. Though, NV7, NV8, NV11, and NV14 showed maximum plant growth, and biomass than NV4, NV6, and NV9 without Cr exposure. Even so, NV7 and NV8 displayed a higher reduction in biomass of plants by FW (69.9/58.3%), DW (78.3/71.8%), SL (72.7/67.5%), RL (75.9/73.1%), correspondingly. However, the genotypes NV11, and NV14 showed a minimum reduction in plant biomass attributes by FW (43.6/48.3%), DW (25.1/31.4%), SL (39/2/40.7%), RL (33.9/37.5%), individually. Moreover, other genotypes represented modest responses against Cr disclosure.

In the case of hybrid varieties, HV3, HV5, HV6, HV9, HV10, and HV14 signified the greater plant biomass i.e., FW, DW, SL, and RL as compared to the other cultivars. Whereas, the HV1 and HV8 showed significantly lowered plant biomass under normal conditions. Under Cr disclosure, HV3, and HV14 cultivars demonstrated the lower reduction in plant biomass by FW (32.9/27.5%), DW (31.2/21.0%), SL (37.2/33.6%), RL (35.4/26.9%), respectively (Table 3). Nonetheless, HV5, and HV10 cultivars showed conspicuous reduction inside plant biomass such as FW (73.5/66.6%), DW (81.3/79.2%), SL (72.3/73.9%), RL (83.4/86.9%), respectively (Table 3). However, other varieties represented a moderate reduction than these above-mentioned cultivars. Our outcomes revealed that the maximum plant biomass was reduced in NV7, NV8 (normal type), and HV5, HV10 (hybrid type) varieties, although minimum biomass reduction was noticed in NV11, NV14 (normal varieties), and HV3, HV14 (hybrid type) cultivars.

3.3. Effect of chromium stress on phenotypic observation

Relying on seed germination indices, and plant biomass attributes, total 4 varieties such as 2 from each rice type as per normal varieties (NV7; sensitive, NV11; tolerant), and hybrid cultivars (HV5; sensitive, HV14; tolerant) were selected to measure the further physiological traits. In the current study, no phenotypic changes were observed under control conditions. The visible length of all four varieties (shoot, and roots) were virtually similar, and plants were healthier. In contrast, significant phenotypical changes were observed under the Cr stress treatment relative to the plants without Cr stress (Fig. S1). The higher reduction in plant height was noticed visually inside HV10, and NV7 rice varieties, especially HV10 being more affected. Although, NV11 and HV14 rice cultivars were noticed with greater height when compared

Table 3
Effect of chromium toxicity on biomass of 14 normal rice types. Fresh weight (g), dry weight (g), shoot length (SL), and root length (RL).

Varieties	FW	DW	RL	SL
NV1-CK	0.90 ± 0.01efg	0.09 ± 0.00 h	14.15 ± 0.06 l	19.98 ± 0.15e
NV1-Cr	0.33 ± 0.01 *m*	0.04 ± 0.00*n*	9.83 ± 0.10o	7.40 ± 0.14 *m*
NV2-CK	0.80 ± 0.46 g	0.13 ± 0.00d	16.43 ± 0.10 g	18.53 ± 0.17 g
NV2-Cr	0.42 ± 0.01jklm	0.06 ± 0.00 k	9.43 ± 0.10p	6.30 ± 0.08o
NV3-CK	0.88 ± 0.02efg	0.07 ± 0.00 k	16.13 ± 0.10i	19.13 ± 0.05f
NV3-Cr	0.51 ± 0.01jk	0.05 ± 0.00 lm	13.30 ± 0.14 *m*	8.58 ± 0.21 k
NV4-CK	1.08 ± 0.01bc	0.12 ± 0.00 fg	19.13 ± 0.05d	20.18 ± 0.13d
NV4-Cr	0.50 ± 0.01jk	0.05 ± 0.00 lm	13.20 ± 0.08 *m*	7.73 ± 0.13 l
NV5-CK	0.98 ± 0.02cde	0.12 ± 0.00ef	17.23 ± 0.10f	17.38 ± 0.15i
NV5-Cr	0.49 ± 0.01jk	0.05 ± 0.00kl	14.40 ± 0.18 k	7.35 ± 0.06 *m*
NV6-CK	0.98 ± 0.01cde	0.15 ± 0.00b	18.13 ± 0.10e	20.08 ± 0.10de
NV6-Cr	0.33 ± 0.01 *m*	0.05 ± 0.00 lm	12.35 ± 0.13*n*	8.33 ± 0.17 k
NV7-CK	1.03 ± 0.01bcd	0.14 ± 0.00c	20.13 ± 0.05c	20.25 ± 0.13c
NV7-Cr	0.31 ± 0.00*n*	0.03 ± 0.00*n*	6.20 ± 0.08 s	5.23 ± 0.10q
NV8-CK	0.92 ± 0.01def	0.14 ± 0.00c	19.23 ± 0.10d	20.43 ± 0.10c
NV8-Cr	0.41 ± 0.01klm	0.04 ± 0.00op	7.73 ± 0.17r	6.35 ± 0.13p
NV9-CK	1.15 ± 0.01b	0.12 ± 0.00ef	24.28 ± 0.05a	21.30 ± 0.08b
NV9-Cr	0.54 ± 0.02ij	0.06 ± 0.00j	16.18 ± 0.13i	7.13 ± 0.17*n*
NV10-CK	0.84 ± 0.01 fg	0.09 ± 0.00 h	20.65 ± 0.13b	18.15 ± 0.10 h
NV10-Cr	0.42 ± 0.02jklm	0.04 ± 0.00op	12.35 ± 0.13*n*	7.70 ± 0.14 l
NV11-CK	1.33 ± 0.02a	0.16 ± 0.00a	15.25 ± 0.10j	22.20 ± 0.08a
NV11-Cr	0.69 ± 0.01 h	0.12 ± 0.00ef	12.20 ± 0.08*n*	17.43 ± 0.17i
NV12-CK	0.83 ± 0.01 fg	0.08 ± 0.00i	20.13 ± 0.10c	17.23 ± 0.10 *m*
NV12-Cr	0.35 ± 0.02 lm	0.04 ± 0.00op	9.68 ± 0.17o	7.35 ± 0.13 *m*
NV13-CK	0.99 ± 0.01cde	0.11 ± 0.00 g	16.40 ± 0.08gh	18.65 ± 0.06 g
NV13-Cr	0.48 ± 0.01jkl	0.04 ± 0.00op	9.23 ± 0.17q	7.33 ± 0.17 *m*
NV14-CK	1.33 ± 0.01a	0.15 ± 0.00b	20.25 ± 0.13c	19.23 ± 0.10f
NV14-Cr	0.67 ± 0.02 h	0.09 ± 0.00 k	16.25 ± 0.06hi	13.78 ± 0.10j

The same letters within a column designate there was no significant difference at a 95% probability level at the $p < 0.05$ level, correspondingly.

to the HV10, and NV7, but the cultivar HV14 represented maximum height s compared to the NV11 (Fig. S1).

3.4. Effect of chromium stress on photosynthetic attributes of rice plants

Under control conditions, there was no more significant difference between chlorophyll contents (Chlorophyll *a*, b, a + b, carotenoids) of four different rice cultivars, but HV10 and HV14 showed a significantly higher level of chlorophyll *a*, and a + b by 9.7/10.2%, and 10.6/11.2%, respectively than NV7 genotype (Fig. 1a-d). Under stressed conditions, the HV14 cultivar represented significantly greater chlorophyll contents as compared to the other genotypes, and more reduction in photosynthetic pigments was noticed in HV10 cultivars (Fig. 1a-d). HV10 cultivar demonstrated the Chlorophyll *a*, b, a + b, carotenoids contents reduction by 57.6%, 79.8%, 58.8%, and 52.7%, NV7 by 49.9%, 71.6%, 47.9%, and 46.7%, NV11 by 18.2%, 32.5%, 19.6%, and 35.8% as well as HV14 by 13.2%, 24.6%, 13.5%, and 27.7%, respectively relative to their controls under Cr-induced toxicity (Fig. 1a-d). Our results displayed that the HV14 cultivar was less affected through the Cr disclosure, and more decrease in chlorophyll contents levels was observed in HV10.

3.5. Effect of chromium stress on total soluble sugar, and electrolyte leakage of rice plants

In untreated plants, the significant difference was not noticed inside the values of total soluble sugar (TSS) amongst all four cultivars of rice. Related to the stressed environment, total soluble sugar was reduced 6.34%, 50.4%, 33.3%, and 25.4% in HV10, NV7, NV11, and NV14, respectively. In contrast, the reverse trend was noticed in the case of electrolyte leakage. The electrolyte leakage (EL) was observed minor in the case of NV14 cultivar by 14.1%. Conversely, the level of EL was markedly higher in the case of HV10, and NV7 by 69.2%, and 57.8%, correspondingly than NV11 (34.7%). Our outcomes revealed that HV14 was lower affected by the Cr-induced toxicity, while HV10 was affected the most under Cr disclosure.

3.6. Quantification of MDA, H_2O_2, and $O_2^{\bullet -}$ contents

The assay was conducted out to observe the oxidative damage caused inside rice cultivars. There was no significant difference inside the values of MDA contents, H_2O_2, and $O_2^{\bullet -}$ production under normal conditions (Fig. 3a-c). Relative to the Cr treated plants, the enhancement inside the values of MDA contents were noticed in HV10, NV7, NV11, and NV14 cultivars by 79.1%, 76.2%, 63.7%, and 43.5%, H_2O_2 by 71.9%, 67.5%, 51.5%, and 49.3%, and $O_2^{\bullet -}$ by 53.8%, 49.2%, 34.6%, and 27.8%, correspondingly (Fig. 3a-c). Our results verified that the significant increase in the values of MDA contents, H_2O_2, and $O_2^{\bullet -}$ were observed in Cr-sensitive varieties (HV10, NV7), although this increment was slightly low inside the Cr-tolerant cultivars (HV14, NV11) of rice, especially in HV14 being more tolerant (Fig. 3a-c).

3.7. Determination of antioxidant enzymatic activities in rice cultivars under Cr stress

The antioxidative activities of enzymes viz., SOD, CAT, POD, and APX were also affected in rice cultivars due to the exposure to Cr stress. The increase was noticed inside the enzymatic activities of rice cultivars. This increment was more obvious inside the values SOD, CAT, POD, and APX in high Cr-tolerant cultivars HV14, and NV11 by 51.2/45.6%, 67.4/61.8%, 75.7/72.5%, and 47.9/42.6%, respectively. Whereas, this increase was slightly lower in less Cr-tolerant cultivars i.e., HV10, and NV7 by 32.5/37.8%, 45.9/51.3%, 53.2/61.4%, and 34.1/39.8%, correspondingly under Cr disclosure (Fig. 4a-c). Our findings indicated that the antioxidative activities (SOD, CAT, POD, and APX) were enhanced under Cr-induced stress,

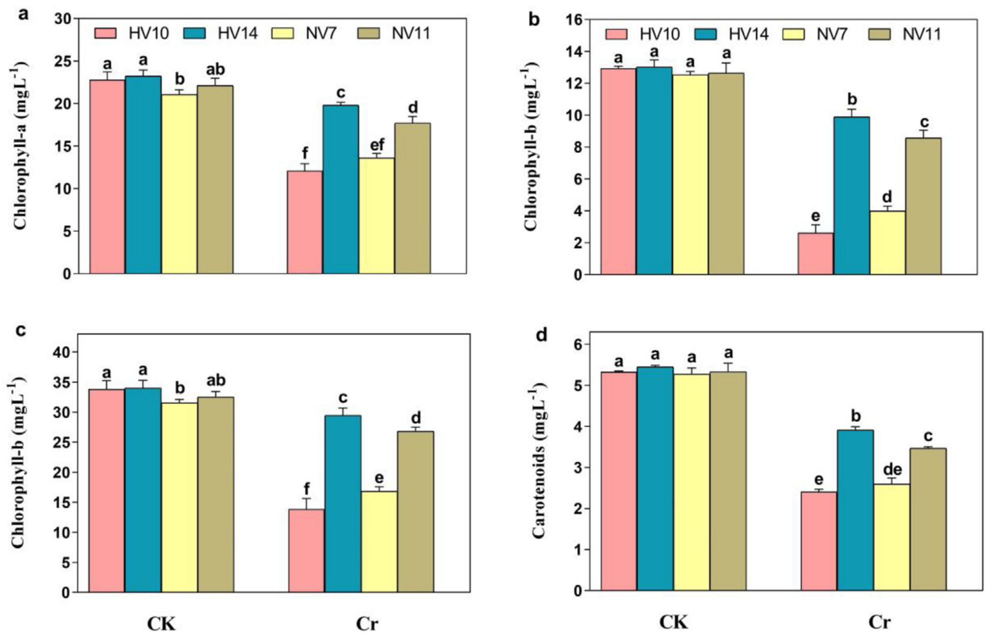

Fig. 1. Photosynthetic pigments of four different rice cultivars with, and without Cr stress. **a** Chlorophyll-a, **b** chlorophyll-b, **c** chlorophyll-a + b, **d** carotenoids. The values shown are the mean standard deviation (n = 4). Treatments with different letters have statistically different values (P < 0.05).

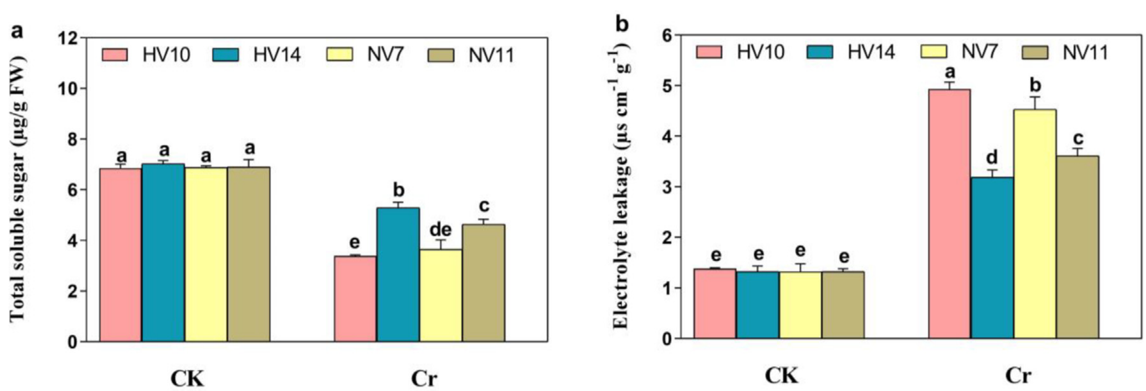

Fig. 2. Determination of total soluble sugar, and electrolyte leakage of four different rice cultivars with, and without Cr stress. **a** total soluble sugar, and **b** electrolyte leakage. The values shown are the mean standard deviation (n = 4). Treatments with different letters have statistically different values (P < 0.05).

but this increase was clearer in Cr-tolerant cultivars, especially in HV14 as compared to the Cr-sensitive cultivars, particularly in HV10. Although, no significant difference in the values of SOD, CAT, POD was noticed inside the plants of all cultivars under control conditions (Fig. 4a-c).

4. Discussion

The increasing level of heavy metal contamination, specifically chromium (Cr), in air, soil, and water is a major source of concern for scientists these days. Plants show various symptoms against Cr toxicity including inhibition of plant growth, leaves color turning yellow, and reduction in biomass of plants, etc. (Singh et al., 2013; Basit et al., 2021a). Rice is a valuable crop that is susceptible to Cr toxicity (Mukta et al., 2019; Basit et al., 2021b: Sharma et al., 2022). Screening rice cultivars by seed germination ratio and Cr-tolerant cultivars based on morpho-physiological traits, and plant biomass under Cr stress would help us better understand the Cr tolerance mechanism in rice, which is yet unclear.

Cr (100 µM) stress exposure caused the inhibition of plants growth, and biomass. The plants roots were inhibited under Cr toxicity, especially in the HV10 cultivar (Tables 3 and 4). It might have happened because the roots are the primary source that comes in contact with the heavy metal contamination (Ganesh et al., 2008; Basit et al., 2022). First, plants uptake Cr contents through the nutrient solution, it accumulates inside roots, and it may decrease the polysaccharide inside the roots cell wall which further causes cellular elongation restriction and later-stage plant growth and development damage (Alam et al., 2021; Terzi and Yıldız, 2021; Ao et al., 2022). The reduction in plant height was clearer in cultivar HV10, and NV7 (Tables 3 and 4). The varieties NV11 and HV14 were represented less inhibition in plant growth, especially HV14 variety was being more tolerant with less reduction in plant

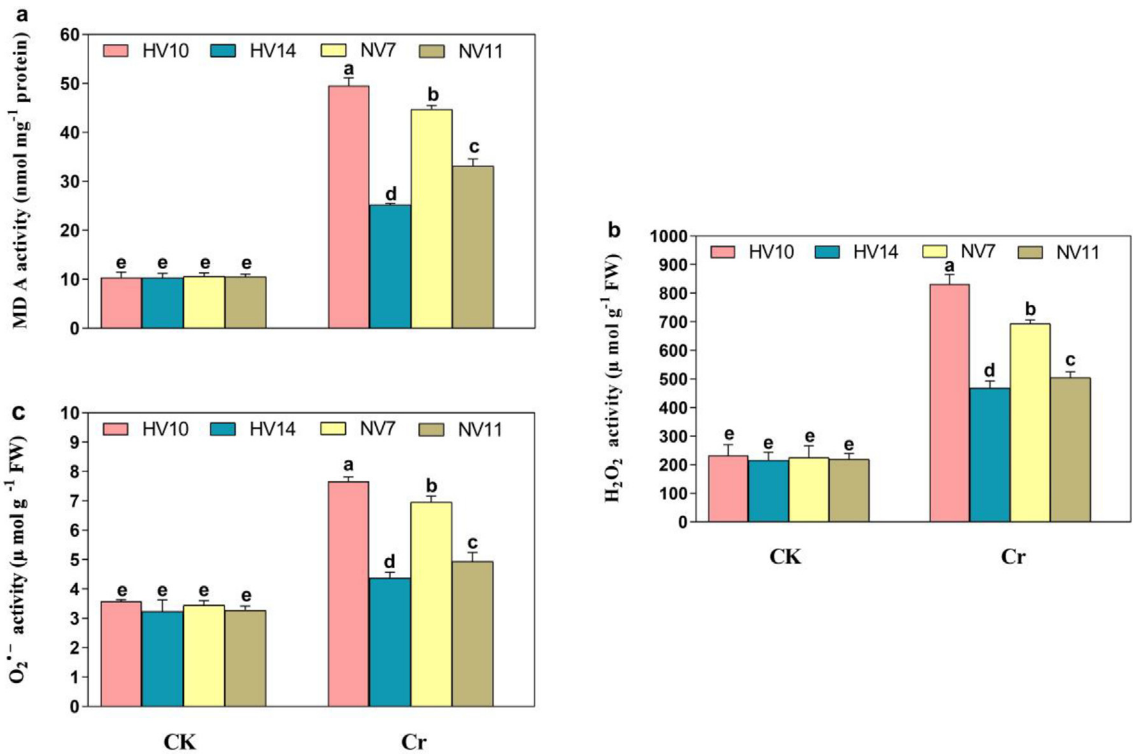

Fig. 3. MDA contents, and ROS accumulation of four different rice cultivars with, and without Cr stress. **a** MDA contents in 4 different rice cultivars. **b** H_2O_2 production in 4 different rice cultivars, and **c** $O_2^{\bullet-}$ contents in 4 different rice cultivars. The values shown are the mean standard deviation (n = 4). Treatments with different letters have statistically different values (P < 0.05).

growth, and biomass reduction. The biomass reduction was more noticeable inside HV10, and NV7 cultivars particularly were more in HV10 as compared to NV7. Probably, Cr-induced damage caused a reduction in cell elongation, and affected the membrane permeability which further imbalanced the nutrient uptake by fluctuating the osmotic balance, and consequently compromised the photosynthetic levels, and plants growth, biomass was also deprived (Naz et al., 2021). The same outcomes were observed inside the *Zea mays* (Naz et al., 2021), *Lycopersicon esculentum* (Alam et al., 2021), and *Vigna radiata* (Husain et al., 2021), and *Brassica nigra* (Akhtar et al., 2021).

It is also reported that the reduction in plant biomass and growth attributes are also directly related to the impairment in the photosynthetic system (Ulhassan et al., 2019a; Ao et al., 2022; Kharbech et al., 2022). As expected, the Cr stress caused the reduction in chlorophyll contents (chlorophyll-a, b, a + b, and carotenoids) of all rice cultivars (Fig. 1a-d), especially HV10 was being more affected. The reduction in chlorophyll contents may be instigated by minimizing the biosynthetic enzyme capability under Cr toxicity (Ulhassan et al., 2019b; Chen et al., 2022). This inhibition of photosynthetic pigments was relatively low inside cultivar HV14, possibly it regulated the chlorophyll pigments related biosynthetic pathways, and activities of heme-based enzymes which are involved in the biosynthesis of chlorophyll contents (Dixit et al., 2002). It is observed that photosynthetic efficiency is known to regulate the quantities of total soluble protein and soluble sugar under stressed conditions (Rizwan et al., 2019). Likewise, the decrease in photosynthesis reduced the total soluble sugar level under Cr stress (Fig. 2a), especially in the HV10 cultivar. Nevertheless, the cultivar HV14 built a specific mechanism to maintain the level of photosynthetic pigments, and total soluble sugar under Cr-induced damage (Fig. 2). It might be occurred by modulating the energy, and transduction mechanism which further upsurged the level of total soluble sugar via improving photosynthetic attributes (Handa et al., 2019; Mukta et al., 2019; Ulhassan et al., 2019a).

In a recent study, the exposure of Cr caused higher production of ROS (H_2O_2, $O_2^{\bullet-}$), and MDA contents, and electrolyte leakage as well in rice cultivars, especially in HV10 than NV7, and NV11. It verified that Cr-induced damage caused higher cellular oxidative damage, exaggerated the membrane damage, and lipid peroxidation in plants. Several studies demonstrated similar results related to Cr caused above-mentioned oxidative markers inside rapeseed (Ulhassan et al., 2019a), *Oryza sativa* (Basit et al., 2021a), *Brassica juncea* (Handa et al., 2019), *Camellia sinensis* (Barman et al., 2020), and *Zea mays* (Kharbech et al., 2020). However, NV14 showed a lower accumulation of ROS and MDA contents (Fig. 3a-c) with a minimum level of electrolyte leakage (Fig. 2b). Most probably, it built a Cr-detoxification mechanism, which reduced oxidative stress and ultimately improved the photosynthetic capabilities. It further lowered the electrolyte leakage and provided membrane stability, and production by reducing the ROS extra-generation, and accumulation (Adhikari et al., 2020; Devi and Kumar, 2020; Basit et al., 2022). Earlier investigations also supported the outcomes obtained from a recent study that plants build some mechanism to uphold the cellular metabolism by lowering the generation of free radicals that eventually reduce the ROS, and MDA levels as well as electrolyte leakage.

To reduce the effect of oxidative damage caused by ROS, and MDA contents higher accumulation under Cr toxicity, plants develop a particular mechanism known as the antioxidative defense mechanism. In the present research, rice cultivars upsurged the enzymatic antioxidative activities against Cr-induced oxidative damage (Fig. 4a-c). It revealed that plants stimulated the antioxidative mechanism to scavenge the extra-accumulated ROS inside plant tissues, which was further increasing MDA con-

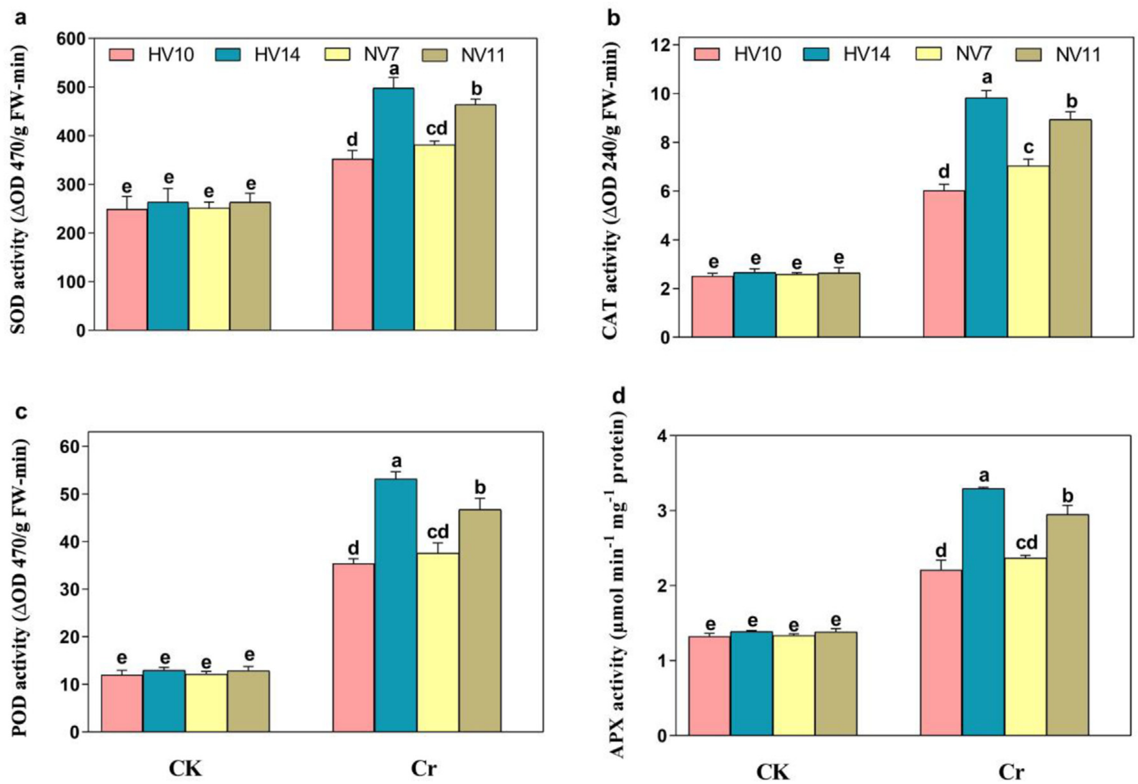

Fig. 4. Antioxidative enzyme activities of four different rice cultivars with, and without Cr stress. **a** SOD 4 different rice cultivars, **b** CAT in 4 different rice cultivars, **c** POD in 4 different rice cultivars, and **d** APX in 4 different rice cultivars. The values shown are the mean standard deviation (n = 4). Treatments with different letters have statistically different values (P < 0.05).

Table 4
Effect of chromium toxicity on biomass of 14 hybrid rice types. Fresh weight (g), dry weight (g), shoot length (SL), and root length (RL).

Varieties	FW	DW	RL	SL
HV1-CK	0.90 ± 0.01efg	0.09 ± 0.00 h	14.15 ± 0.06 l	19.98 ± 0.15e
HV1-Cr	0.33 ± 0.01 m	0.04 ± 0.00n	9.83 ± 0.10o	7.40 ± 0.14 m
HV2-CK	0.80 ± 0.46 g	0.13 ± 0.00d	16.43 ± 0.10 g	18.53 ± 0.17 g
HV2-Cr	0.42 ± 0.01jklm	0.06 ± 0.00 k	9.43 ± 0.10p	6.30 ± 0.08o
HV3-CK	0.88 ± 0.02efg	0.07 ± 0.00 k	16.13 ± 0.10i	19.13 ± 0.05f
HV3-Cr	0.51 ± 0.01jk	0.05 ± 0.00 lm	13.30 ± 0.14 m	8.58 ± 0.21 k
HV4-CK	1.08 ± 0.01bc	0.12 ± 0.00 fg	19.13 ± 0.05d	20.18 ± 0.13d
HV4-Cr	0.50 ± 0.01jk	0.05 ± 0.00 lm	13.20 ± 0.08 m	7.73 ± 0.13 l
HV5-CK	0.98 ± 0.02cde	0.12 ± 0.00ef	17.23 ± 0.10f	17.38 ± 0.15i
HV5-Cr	0.49 ± 0.01jk	0.05 ± 0.00kl	14.40 ± 0.18 k	7.35 ± 0.06 m
HV6-CK	0.98 ± 0.01cde	0.15 ± 0.00b	18.13 ± 0.10e	20.08 ± 0.10de
HV6-Cr	0.33 ± 0.01 m	0.05 ± 0.00 lm	12.35 ± 0.13n	8.33 ± 0.17 k
HV7-CK	1.03 ± 0.01bcd	0.14 ± 0.00c	20.13 ± 0.05c	20.25 ± 0.13c
HV7-Cr	0.31 ± 0.00n	0.03 ± 0.00n	6.20 ± 0.08 s	5.23 ± 0.10q
HV8-CK	0.92 ± 0.01def	0.14 ± 0.00c	19.23 ± 0.10d	20.43 ± 0.10c
HV8-Cr	0.41 ± 0.01klm	0.04 ± 0.00op	7.73 ± 0.17r	6.35 ± 0.13p
HV9-CK	1.15 ± 0.01b	0.12 ± 0.00ef	24.28 ± 0.05a	21.30 ± 0.08b
HV9-Cr	0.54 ± 0.02ij	0.06 ± 0.00j	16.18 ± 0.13i	7.13 ± 0.17n
HV10-CK	0.84 ± 0.01 fg	0.09 ± 0.00 h	20.65 ± 0.13b	18.15 ± 0.10 h
HV10-Cr	0.42 ± 0.02jklm	0.04 ± 0.00op	12.35 ± 0.13n	7.70 ± 0.14 l
HV11-CK	1.33 ± 0.02a	0.16 ± 0.00a	15.25 ± 0.10j	22.20 ± 0.08a
HV11-Cr	0.69 ± 0.01 h	0.12 ± 0.00ef	12.20 ± 0.08n	17.43 ± 0.17i
HV12-CK	0.83 ± 0.01 fg	0.08 ± 0.00i	20.13 ± 0.10c	17.23 ± 0.10 m
HV12-Cr	0.35 ± 0.02 lm	0.04 ± 0.00op	9.68 ± 0.17o	7.35 ± 0.13 m
HV13-CK	0.99 ± 0.01cde	0.11 ± 0.00 g	16.40 ± 0.08gh	18.65 ± 0.06 g
HV13-Cr	0.48 ± 0.01jkl	0.04 ± 0.00op	9.23 ± 0.17q	7.33 ± 0.17 m
HV14-CK	1.33 ± 0.01a	0.15 ± 0.00b	20.25 ± 0.13c	19.23 ± 0.10f
HV14-Cr	0.67 ± 0.02 h	0.09 ± 0.00 k	16.25 ± 0.06hi	13.78 ± 0.10j

The same letters within a column designate there was no significant difference at a 95% probability level at the p < 0.05 level, correspondingly.

tents (Fig. 3a-c, 4a-d). The greater stimulation inside the above-mentioned antioxidative markers was also documented in *Oryza sativa* (Basit et al., 2021a; Yang et al., 2021), *Zea mays* (Anjum et al., 2016; Danish et al., 2019), and *Triticum aestivum* (Anjum et al., 2016). The level of enzymatic activities was prominently enhanced by the HV14 cultivar as compared to the NV7, NV11, and specifically HV10. Possibly, it maintained the redox balance which further reduce the excessive accumulation of ROS inside cellular compartments of plants under Cr contaminated environment. The suggested mechanism illustrates a crucial strategy of a Cr-tolerant cultivar (HV14), used to eradicate the Cr stress in plants.

5. Conclusion

Our outcomes revealed that NV4, NV7, NV8, NV9, NV11, and NV14 (normal type) cultivars as well as HV2, HV3, HV5, HV9, HV10, and HV14 (hybrid type) varieties showed maximum germination vigor under control conditions. Whereas 28 different rice cultivars (NV1-NV14, HV1-HV14) were exposed to chromium (Cr) toxicity, plant biomass was significantly reduced. NV2, NV6, NV10, NV12, NV13 (normal varieties), HV1, HV4, HV8, and HV9 (hybrid types) were identified as moderately sensitive varieties, whereas NV3, NV4, NV9, and NV14 (normal types), HV3, HV6, HV7, and HV13 were identified as moderately tolerant varieties. While, compared to the other rice genotypes (both groups; normal, and hybrid), the most susceptible cultivars were NV7 and HV10, even though the most tolerant cultivars were NV11 and HV14. Moreover, the tolerant cultivars demonstrated the tolerant mechanism in contrast to Cr-sensitive cultivars. In addition, Cr-tolerant varieties improved the chlorophyll contents by lowering the ROS accumulation, and MDA production via stimulating the antioxidative enzyme activities, which further enhanced the total soluble sugar, and minimized the electrolyte leakage in rice Cr-tolerant cultivars. Resultantly, plant biomass and growth were improved in Cr-tolerant varieties as compared to the Cr-sensitive cultivars. By getting an understanding of the Cr-tolerant mechanism, researchers would be able to build a systematic strategy to overcome the heavy metal stress in agricultural soil.

Ethics approval

Not applicable.

Consent to participate

All authors consent to participate in the manuscript publication.

6. Consent for publication

All authors approved the manuscript to be published.

7. Availability of data and material

All data and materials as well as software application or custom code support our claims and comply with field standards. All data generated or analyzed during this study are included in this published article.

Funding

The authors have no relevant financial or non-financial interests to disclose.

Author contribution

YG, JAB and JH are involved in conceptualization, YG, JAB and FB design experiment. FB, JH performed experiment and writing manuscript. FB, JAB and JH writing and editing assistance the manuscript. BLJ, AS and SA analyzed the data and also revised the manuscript. All authors read and approved the final manuscript.

Declaration of Competing Interest

The authors declare that they have no known competing financial interests or personal relationships that could have appeared to influence the work reported in this paper.

Acknowledgement

This research was supported by National Natural Science Foundation of China (No. 32072127), Zhejiang Provincial Natural Science Foundation (No. LY21C130006), Dabeinong Funds for Discipline Development and Talent Training in Zhejiang University, Collaborative Innovation Center for Modern Crop Production co-sponsored by Province and Ministry (CIC-MCP) and Zhenjiang International-joint fund (No. GJ2020010). The authors would like to extend their sincere appreciation to the Researchers Supporting Project Number (RSP-2021/168), King Saud University, Riyadh, Saudi Arabia.

Appendix A. Supplementary material

Supplementary data to this article can be found online at https://doi.org/10.1016/j.sjbs.2022.02.038.

References

Adhikari, A., Adhikari, S., Ghosh, S., Azahar, I., Shaw, A.K., Roy, D., Roy, S., Saha, S., Hossain, Z., 2020. Imbalance of redox homeostasis and antioxidant defense status in maize under chromium (VI) stress. Environmental and Experimental Botany 169, 103873. https://doi.org/10.1016/j.envexpbot.2019.103873.

Akhtar, N., Ilyas, N., Yasmin, H., Sayyed, R., Hasnain, Z., A Elsayed, E., El Enshasy, H.A., 2021. Role of Bacillus cereus in Improving the Growth and Phytoextractability of *Brassica nigra* (L.) K. Koch in Chromium Contaminated Soil. Molecules, 26, 1569.

Al-Huqail, A.A., Ali, H.M., Kushwaha, B.K., AL-Huqail, A.A., Singh, V.P., Siddiqui, M.H., 2020. Ascorbic acid is essential for inducing chromium (VI) toxicity tolerance in tomato roots. Journal of Biotechnology 322, 66–73.

Alam, P., Balawi, T.H., Altalayan, F.H., Hatamleh, A.A., Ashraf, M., Ahmad, P., 2021. Silicon attenuates the negative effects of chromium stress in tomato plants by modifying antioxidant enzyme activities, ascorbate–glutathione cycle and glyoxalase system. Acta Physiologiae Plantarum 43, 1–17.

Alamri, S., Ali, H.M., Khan, M.I.R., Singh, V.P., Siddiqui, M.H., 2020. Exogenous nitric oxide requires endogenous hydrogen sulfide to induce the resilience through sulfur assimilation in tomato seedlings under hexavalent chromium toxicity. Plant Physiology and Biochemistry 155, 20–34.

Anjum, S.A., Ashraf, U., Khan, I., Tanveer, M., Saleem, M.F., Wang, L., 2016. Aluminum and chromium toxicity in maize: implications for agronomic attributes, net photosynthesis, physio-biochemical oscillations, and metal accumulation in different plant parts. Water, Air, & Soil Pollution 227, 1–14.

Ao, M., Chen, X., Deng, T., Sun, S., Tang, Y., Morel, J.L., Qiu, R., Wang, S., 2022. Chromium biogeochemical behaviour in soil-plant systems and remediation strategies: A critical review. Journal of Hazardous Materials. 424, 127233. https://doi.org/10.1016/j.jhazmat.2021.127233.

Ashraf, A., Bibi, I., Niazi, N.K., Ok, Y.S., Murtaza, G., Shahid, M., Kunhikrishnan, A., Li, D., Mahmood, T., 2017. Chromium (VI) sorption efficiency of acid-activated banana peel over organo-montmorillonite in aqueous solutions. International journal of phytoremediation 19 (7), 605–613.

Barman, T., Barooah, A.K., Goswami, B.C., Sharma, N., Panja, S., Khare, P., Karak, T., 2020. Contents of chromium and arsenic in tea (*Camellia sinensis* L.): extent of transfer into tea infusion and health consequence. Biological trace element research 196 (1), 318–329.

Basit, F., Chen, M., Ahmed, T., Shahid, M., Noman, M., Liu, J., An, J., Hashem, A., Fahad Al-Arjani, A.-B., Alqarawi, A.A., Alsayed, M.F.S., Fathi Abd_Allah, E., Hu, J., Guan, Y., 2021a. Seed priming with brassinosteroids alleviates chromium stress in rice cultivars via improving ROS metabolism and antioxidant defense response at biochemical and molecular levels. Antioxidants 10 (7), 1089. https://doi.org/10.3390/antiox10071089.

Basit, F., Liu, J., An, J., Chen, M., He, C., Zhu, X., Li, Z., Hu, J., Guan, Y., 2021b. Brassinosteroids as a multidimensional regulator of plant physiological and molecular responses under various environmental stresses. Environmental Science and Pollution Research 28 (33), 44768–44779.

Basit, F., Liu, J., An, J., Chen, M., He, C., Zhu, X., Li, Z., Hu, J., Guan, Y., 2021c. Seed priming with brassinosteroids alleviates aluminum toxicity in rice via improving antioxidant defense system and suppressing aluminum uptake. Environmental Science and Pollution Research, 1–15.

Basit, F., Ulhassan, Z., Mou, Q., Nazir, M.M., Hu, J., Hu, W., Song, W., Sheteiwy, M.S., Zhou, W., Bhat, J.A., Jeddi, K., Hessini, K., Guan, Y., 2022. Seed priming with nitric oxide and/or spermine mitigate the chromium toxicity in rice (*Oryza sativa*) seedlings by improving the carbon-assimilation and minimising the oxidative damages. Functional Plant Biology. https://doi.org/10.1071/FP21268.

Change, B., Maehly, A., 1955. Assay of catalases and peroxidase. Methods Enzymol 2, 764–775.

Chen, F.u., Muhammad, F.G., Khan, Z.I., Ahmad, K., Nadeem, M., Mahmood, S., Awan, M.U.F., Munir, M., Malik, I.S., Ashfaq, A., Sultana, R., Maqsood, A., Saqlain, L., Naeem, M., Ma, J., 2022. Ecological risk assessment of heavy metal chromium in a contaminated pastureland area in the central punjab, pakistan: Soils vs plants vs ruminants. Environ Sci Pollut Res 29 (3), 4170–4179.

Chhogyell, N., Pradhan, N., Ghimiray, M., Bajgai, Y., 2016. Evaluation of short duration rice *(Oryza sativa)* varieties as a strategy to cope with climate change. Proc Bhutan Ecol Soc 1, 91–103.

Danish, S., Kiran, S., Fahad, S., Ahmad, N., Ali, M.A., Tahir, F.A., Rasheed, M.K., Shahzad, K., Li, X., Wang, D., Mubeen, M., Abbas, S., Munir, T.M., Hashmi, M.Z., Adnan, M., Saeed, B., Saud, S., Khan, M.N., Ullah, A., Nasim, W., 2019. Alleviation of chromium toxicity in maize by Fe fortification and chromium tolerant ACC deaminase producing plant growth promoting rhizobacteria. Ecotoxicology and environmental safety 185, 109706. https://doi.org/10.1016/j.ecoenv.2019.109706.

Devi, P., Kumar, P., 2020. Effect of bioremediation on internodal length and leaf area of maize plant cultivated in contaminated soil with chromium metal. Journal of Pharmacognosy and Phytochemistry 9, 1408–1413.

Din, B.U., Amna, Rafique, M., Javed, M.T., Kamran, M.A., Mehmood, S., Khan, M., Sultan, T., Hussain Munis, M.F., Chaudhary, H.J., 2020. Assisted phytoremediation of chromium spiked soils by Sesbania Sesban in association with Bacillus xiamenensis PM14: A biochemical analysis. Plant physiology and biochemistry 146, 249–258.

Dixit, V., Pandey, V., Shyam, R., 2002. Chromium ions inactivate electron transport and enhance superoxide generation in vivo in pea (*Pisum sativum* L. cv. Azad) root mitochondria. Plant, Cell & Environment 25, 687–693.

Dubois, M., Gilles, K., Hamilton, J.K., Rebers, P.A., Smith, F., 1951. A colorimetric method for the determination of sugars. Nature 168 (4265), 167.

Economou-Eliopoulos, M., Frei, R., Atsarou, C., 2014. Application of chromium stable isotopes to the evaluation of Cr (VI) contamination in groundwater and rock leachates from central Euboea and the *Assopos basin* (Greece). Catena 122, 216–228.

Farid, M., Ali, S., Rizwan, M., Ali, Q., Abbas, F., Bukhari, S.A.H., Saeed, R., Wu, L., 2017. Citric acid assisted phytoextraction of chromium by sunflower; morpho-physiological and biochemical alterations in plants. Ecotoxicology and environmental safety 145, 90–102.

Farid, M., Ali, S., Saeed, R., Rizwan, M., Bukhari, S.A.H., Abbasi, G.H., Hussain, A., Ali, B., Zamir, M.S.I., Ahmad, I., 2019. Combined application of citric acid and 5-aminolevulinic acid improved biomass, photosynthesis and gas exchange attributes of sunflower (*Helianthus annuus* L.) grown on chromium contaminated soil. International journal of phytoremediation 21 (8), 760–767.

Ganesh, K.S., Baskaran, L., Rajasekaran, S., Sumathi, K., Chidambaram, A.L.A., Sundaramoorthy, P., 2008. Chromium stress induced alterations in biochemical and enzyme metabolism in aquatic and terrestrial plants. Colloids and Surfaces B: Biointerfaces 63 (2), 159–163.

Geng, J., Yin, Y., Liang, Q., Zhu, Z., Luo, H., 2019. Polyethyleneimine cross-linked graphene oxide for removing hazardous hexavalent chromium: Adsorption performance and mechanism. Chemical Engineering Journal 361, 1497–1510.

Gill, R.A., Zhang, N.a., Ali, B., Farooq, M.A., Xu, J., Gill, M.B., Mao, B., Zhou, W., 2016. Role of exogenous salicylic acid in regulating physio-morphic and molecular changes under chromium toxicity in black-and yellow-seeded *Brassica napus* L. Environmental Science and Pollution Research 23 (20), 20483–20496.

Gross, B.L., Zhao, Z., 2014. Archaeological and genetic insights into the origins of domesticated rice. Proceedings of the National Academy of Sciences 111 (17), 6190–6197.

Habiba, U., Ali, S., Rizwan, M., Ibrahim, M., Hussain, A., Shahid, M.R., Alamri, S.A., Alyemeni, M.N., Ahmad, P., 2019. Alleviative role of exogenously applied mannitol in maize cultivars differing in chromium stress tolerance. Environmental Science and Pollution Research 26 (5), 5111–5121.

Handa, N., Kohli, S.K., Sharma, A., Thukral, A.K., Bhardwaj, R., Abd_Allah, E.F., Alqarawi, A.A., Ahmad, P., 2019. Selenium modulates dynamics of antioxidative defence expression, photosynthetic attributes and secondary metabolites to mitigate chromium toxicity in *Brassica juncea* L. plants. Environmental and Experimental Botany 161, 180–192.

Heath, R.L., Packer, L., 1968. Photoperoxidation in isolated chloroplasts: I. Kinetics and stoichiometry of fatty acid peroxidation. Archives of biochemistry and biophysics 125 (1), 189–198.

Hossain, M.A., Hasanuzzaman, M., Fujita, M., 2010. Up-regulation of antioxidant and glyoxalase systems by exogenous glycinebetaine and proline in mung bean confer tolerance to cadmium stress. Physiology and Molecular Biology of Plants 16 (3), 259–272.

Husain, T., Suhel, M., Prasad, S., Singh, V., 2021. Ethylene and hydrogen sulphide are essential for mitigating hexavalent chromium stress in two pulse crops. Plant Biology.

Islam, M.A., Angove, M.J., Morton, D.W., 2019. Recent innovative research on chromium (VI) adsorption mechanism. Environmental Nanotechnology, Monitoring & Management 12, 100267. https://doi.org/10.1016/j.enmm.2019.100267.

Ista, L.K., Callow, M.E., Finlay, J.A., Coleman, S.E., Nolasco, A.C., Simons, R.H., Callow, J.A., Lopez, G.P., 2004. Effect of substratum surface chemistry and surface energy on attachment of marine bacteria and algal spores. Applied and environmental microbiology 70 (7), 4151–4157.

Jiang, M., Zhang, J., 2001. Effect of abscisic acid on active oxygen species, antioxidative defence system and oxidative damage in leaves of maize seedlings. Plant and Cell Physiology, 42, 1265-1273.

Karthikeyan, P., Elanchezhiyan, S.SD., Preethi, J., Meenakshi, S., Park, C.M., 2020. Mechanistic performance of polyaniline-substituted hexagonal boron nitride composite as a highly efficient adsorbent for the removal of phosphate, nitrate, and hexavalent chromium ions from an aqueous environment. Applied Surface Science 511, 145543. https://doi.org/10.1016/j.apsusc.2020.145543.

Kharbech, O., Sakouhi, L., Mahjoubi, Y., Massoud, M.B., Debez, A., Zribi, O.T., Djebali, W., Chaoui, A., Mur, L.A.J., 2022. Nitric oxide donor, sodium nitroprusside modulates hydrogen sulfide metabolism and cysteine homeostasis to aid the alleviation of chromium toxicity in maize seedlings (*Zea mays* L.). Journal of Hazardous Materials.

Kharbech, O., Sakouhi, L., Ben Massoud, M., Jose Mur, L.A., Corpas, F.J., Djebali, W., Chaoui, A., 2020. Nitric oxide and hydrogen sulfide protect plasma membrane integrity and mitigate chromium-induced methylglyoxal toxicity in maize seedlings. Plant Physiology and Biochemistry 157, 244–255.

Kwasniewski, M., Chwialkowska, K., Kwasniewska, J., Kusak, J., Siwinski, K., Szarejko, I., 2013. Accumulation of peroxidase-related reactive oxygen species in trichoblasts correlates with root hair initiation in barley. Journal of plant physiology 170 (2), 185–195.

Lichtenthaler, H.K., Wellburn, A.R., 1983. Determinations of total carotenoids and chlorophylls a and b of leaf extracts in different solvents. Portland Press Ltd.

Moorthy, K.K., Babu, P., Sreedhar, M., Sama, V.S.A.K., Kumar, P.N., Balachandran, S. M., Sundaram, R.M., 2011. Identification of informative EST-SSR markers capable of distinguishing popular Indian rice varieties and their utilization in seed genetic purity assessments. Seed Science and Technology 39 (2), 282–292.

Mosavi, A.A., Jelodar, N.B., Kazemitabar, K., 2013. Environmental responses and stability analysis for grain yield of some rice genotypes. World Applied Sciences Journal, 21, 105-108.

Mukta, R.H., Khatun, M.R., Nazmul Huda, A.K.M., 2019. Calcium induces phytochelatin accumulation to cope with chromium toxicity in rice (*Oryza sativa* L.). Journal of Plant Interactions 14 (1), 295–302.

Nakano, Y., Asada, K., 1981. Hydrogen peroxide is scavenged by ascorbate-specific peroxidase in spinach chloroplasts. Plant and cell physiology 22, 867–880.

Naz, R., Sarfraz, A., Anwar, Z., Yasmin, H., Nosheen, A., Keyani, R., Roberts, T.H., 2021. Combined ability of salicylic acid and spermidine to mitigate the individual and interactive effects of drought and chromium stress in maize (*Zea mays* L.). Plant Physiology and Biochemistry 159, 285–300.

Patra, C., Medisetti, R.M.N., Pakshirajan, K., Narayanasamy, S., 2019. Assessment of raw, acid-modified and chelated biomass for sequestration of hexavalent chromium from aqueous solution using Sterculia villosa Roxb. shells. Environmental Science and Pollution Research 26 (23), 23625–23637.

Rizwan, M., Mostofa, M.G., Ahmad, M.Z., Zhou, Y., Adeel, M., Mehmood, S., Ahmad, M.A., Javed, R., Imtiaz, M., Aziz, O., Ikram, M., Tu, S., Liu, Y., 2019. Hydrogen sulfide enhances rice tolerance to nickel through the prevention of chloroplast damage and the improvement of nitrogen metabolism under excessive nickel. Plant Physiology and Biochemistry 138, 100–111.

Sharma, A., Vishwakarma, K., Singh, N.K., Prakash, V., Ramawat, N., Prasad, R., Sahi, S., Singh, V.P., Tripathi, D.K., Sharma, S., 2022. Synergistic action of silicon nanoparticles and indole acetic acid in alleviation of chromium (crvi) toxicity in oryza sativa seedlings. Journal of 343, 71–82.

Shen, Z., Zhang, Y., McMillan, O., Jin, F., Al-Tabbaa, A., 2017. Characteristics and mechanisms of nickel adsorption on biochars produced from wheat straw pellets and rice husk. Environmental Science and Pollution Research 24 (14), 12809–12819.

Singh, H.P., Mahajan, P., Kaur, S., Batish, D.R., Kohli, R.K., 2013. Chromium toxicity and tolerance in plants. Environmental Chemistry Letters 11 (3), 229–254.

Singh, P., Itankar, N., Patil, Y., 2021. Biomanagement of hexavalent chromium: current trends and promising perspectives. Journal of Environmental Management 279, 111547. https://doi.org/10.1016/j.jenvman.2020.111547.

Singh, S., Prasad, S.M., 2019. Management of chromium (VI) toxicity by calcium and sulfur in tomato and brinjal: implication of nitric oxide. Journal of hazardous materials 373, 212–223.

Terzi, H., Yıldız, M., 2021. Proteomic analysis reveals the role of exogenous cysteine in alleviating chromium stress in maize seedlings. Ecotoxicology and Environmental Safety 209, 111784. https://doi.org/10.1016/j.ecoenv.2020.111784.

Thakur, S., Singh, P.K., Das, A., Rathour, R., Variar, M., Prashanthi, S.K., Singh, A.K., Singh, U.D., Chand, D., Singh, N.K., Sharma, T.R., 2015. Extensive sequence variation in rice blast resistance gene Pi54 makes it broad spectrum in nature. Frontiers in plant science 6. https://doi.org/10.3389/fpls.2015.00345.

Ulhassan, Z., Gill, R.A., Ali, S., Mwamba, T.M., Ali, B., Wang, J., Huang, Q., Aziz, R., Zhou, W., 2019a. Dual behavior of selenium: insights into physio-biochemical, anatomical and molecular analyses of four *Brassica napus* cultivars. Chemosphere 225, 329–341.

Ulhassan, Z., Gill, R.A., Huang, H., Ali, S., Mwamba, T.M., Ali, B., Huang, Q., Hamid, Y., Khan, A.R., Wang, J., Zhou, W., 2019b. Selenium mitigates the chromium toxicity in *Brassicca napus* L. by ameliorating nutrients uptake, amino acids metabolism and antioxidant defense system. Plant Physiology and Biochemistry 145, 142–152.

Wakeel, A., Ali, I., Wu, M., Raza Kkan, A., Jan, M., Ali, A., Liu, Y., Ge, S., Wu, J., liu, B., Gan, Y., 2019. Ethylene mediates dichromate-induced oxidative stress and regulation of the enzymatic antioxidant system-related transcriptome in Arabidopsis thaliana. Environmental and Experimental Botany 161, 166–179.

Wakeel, A., Ali, I., Wu, M., Liu, B., Gan, Y., 2021. Dichromate-induced ethylene biosynthesis, perception, and signaling regulate the variance in root growth inhibition among Shaheen basmati and basmati-385 rice varieties. Environmental Science and Pollution Research 28 (28), 38016–38025.

Wakeel, A., Xu, M., Gan, Y., 2020. Chromium-induced reactive oxygen species accumulation by altering the enzymatic antioxidant system and associated cytotoxic, genotoxic, ultrastructural, and photosynthetic changes in plants. International journal of molecular sciences 21 (3), 728. https://doi.org/10.3390/ijms21030728.

Xu, B.o., Wang, F., Zhang, Q., Lan, Q., Liu, C., Guo, X., Cai, Q., Chen, Y., Wang, G., Ding, J., 2018. Influence of iron plaque on the uptake and accumulation of chromium by rice (*Oryza sativa* L.) seedlings: Insights from hydroponic and soil cultivation. Ecotoxicology and environmental safety 162, 51–58.

Yang, S.u., Ulhassan, Z., Shah, A.M., Khan, A.R., Azhar, W., Hamid, Y., Hussain, S., Sheteiwy, M.S., Salam, A., Zhou, W., 2021. Salicylic acid underpins silicon in ameliorating chromium toxicity in rice by modulating antioxidant defense, ion homeostasis and cellular ultrastructure. Plant Physiology and Biochemistry 166, 1001–1013.

Zaheer, I.E., Ali, S., Saleem, M.H., Noor, I., El-Esawi, M.A., Hayat, K., Rizwan, M., Abbas, Z., El-Sheikh, M.A., Alyemeni, M.N., Wijaya, L., 2020. Iron-Lysine mediated alleviation of chromium toxicity in spinach (*Spinacia oleracea* L.) plants in relation to morpho-physiological traits and iron uptake when irrigated with tannery wastewater. Sustainability 12 (16), 6690. https://doi.org/10.3390/su12166690.

Zheng, Y., Hu, J., Zhang, S., Gao, C., Song, W., 2006. Identification of chilling-tolerance in maize inbred lines at germination and seedling growth stages. Journal of Zhejiang University (Agriculture and Life Science) 32, 41–45.